

The Central Preshower Detector, a core dump of useful information

Ken Del Signore
University of Michigan
1 April 1899

Abstract:

This note is to summarize the design, geometry, and installation of the Central Preshower Detector. A description of the detector system is given along with relevant geometric quantities. Various mechanical and schematic drawings of the system are included for posterity.

Contents:

1. Introduction
2. Detector Structure and Layout.
3. Connector Channel Ordering
4. Installation and final alignment of detector modules.
5. Pre-installation Source Testing.
6. Minutia

1. Introduction

The Central Preshower Detector (CPS) is designed to provide a trigger level response to hi pt electrons within the central tracking volume. The detector consists of three concentric cylindrical layers of triangular scintillator strips, situated between the solenoid and the central calorimeter as seen in Fig.1. The three layers are arranged in an axial-u-v geometry, with a stereo angle of ~23 degrees. In addition, a $1X_0$ Pb radiator is situated between the solenoid and CPS to enhance showering. The total radiation length of the solenoid + Pb is $2X_0$ for particles at normal incidence.

The scintillator strips used for all three layers have an equilateral triangular cross section as shown in Fig. 2. A hole to house a wavelength shifter fiber (WLS) runs the length of the strip. The strips are wrapped in aluminized mylar for optical isolation. Successive strips within each layer are interleaved as seen in Fig. 3. This design gives zero dead space between strips and also provides a vernier effect to showers and mips.

The WLS fibers within each strip are split at $Z=0$, and read out from each end . The non readout ends of the fibers are diamond polished and mirrored to reflect light to the readout end. At the readout end, the fibers are grouped into groups of 16 and potted into connectors for transition to the clear fiber light guides.

The channel count and geometry of the detector is designed to match that of the Central Fiber Tracker (CFT) for Level 1 triggering purposes. The CFT is divided into 80 sectors in phi for L1 track finding. Each group of 16 axial strips (grouped into one WLS connector) corresponds to one CFT sector. The stereo layers are not used at L1, but retain the same channel count as the axial layer. There are thus $80 \text{ sectors} \times 16 \text{ strips/sector} = 1280 \text{ strips/layer}$, and twice this number, 2560, of readout channels/layer.

Section 2 describes the layout and physical makeup of the detector system. Section 3 describes the connector channel ordering, and section 4 documents the final alignment of the detector with respect to the solenoid. Section 5 documents the pre-installation source testing that was preformed on the entire system. The test allows an initial strip to strip calibration, and results are presented. Thorough details of the CPS detector performance, construction procedure, and simulation results can be found in references 1-3, and references therein .

All distances are given in units of inches, unless otherwise stated.

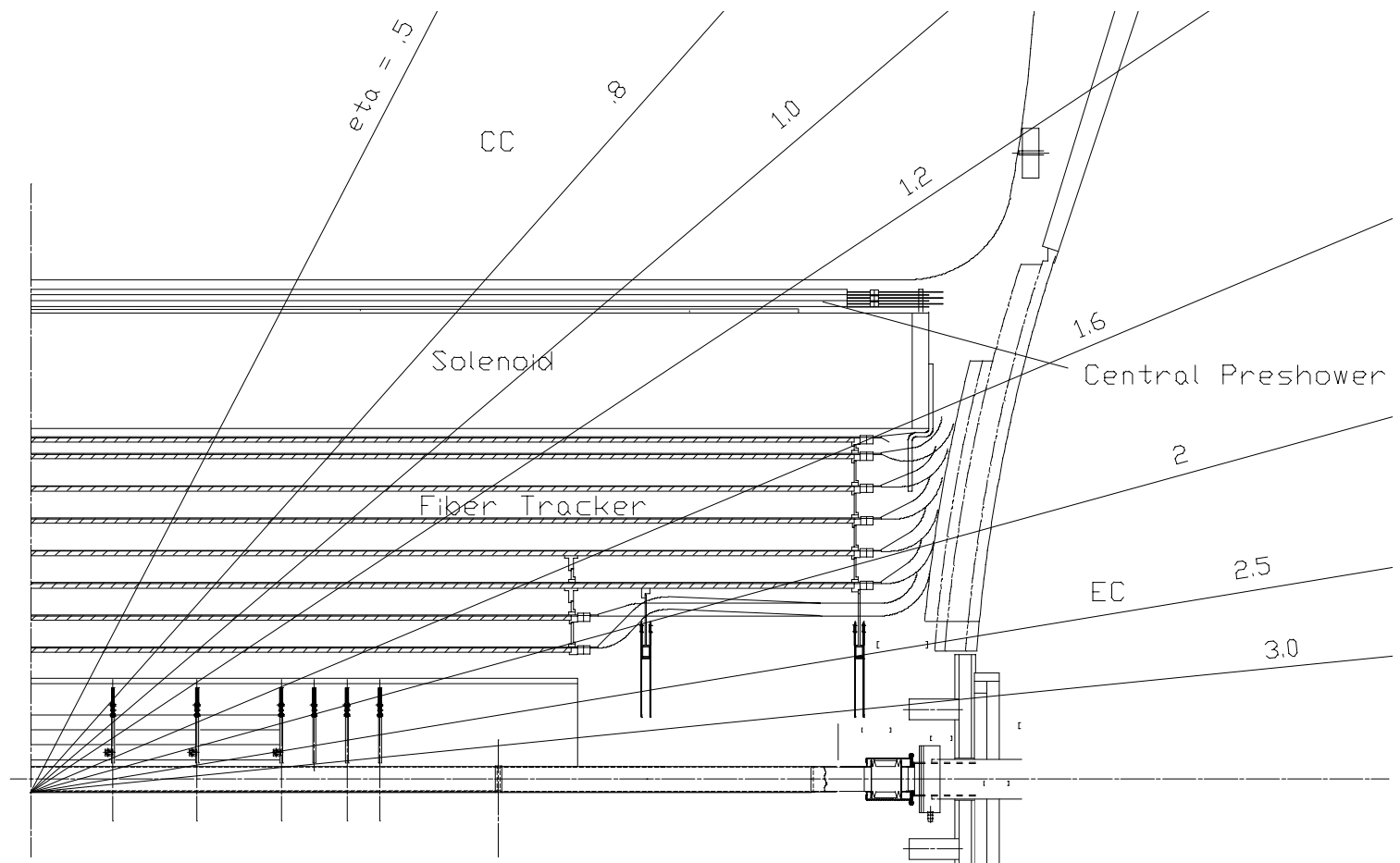


Figure 1. Side view of the D0 central tracking system. CPS detector is located between the Solenoid and Central Calorimeter.

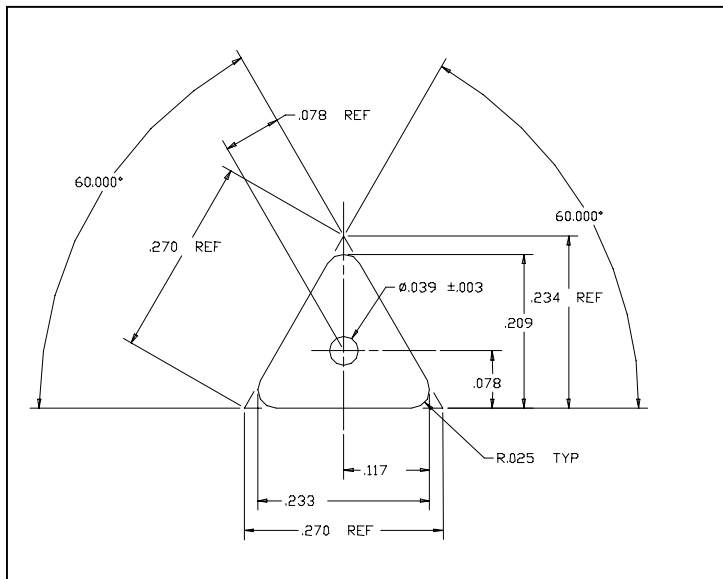


Figure 2. Cross section of the CPS scintillator strip.

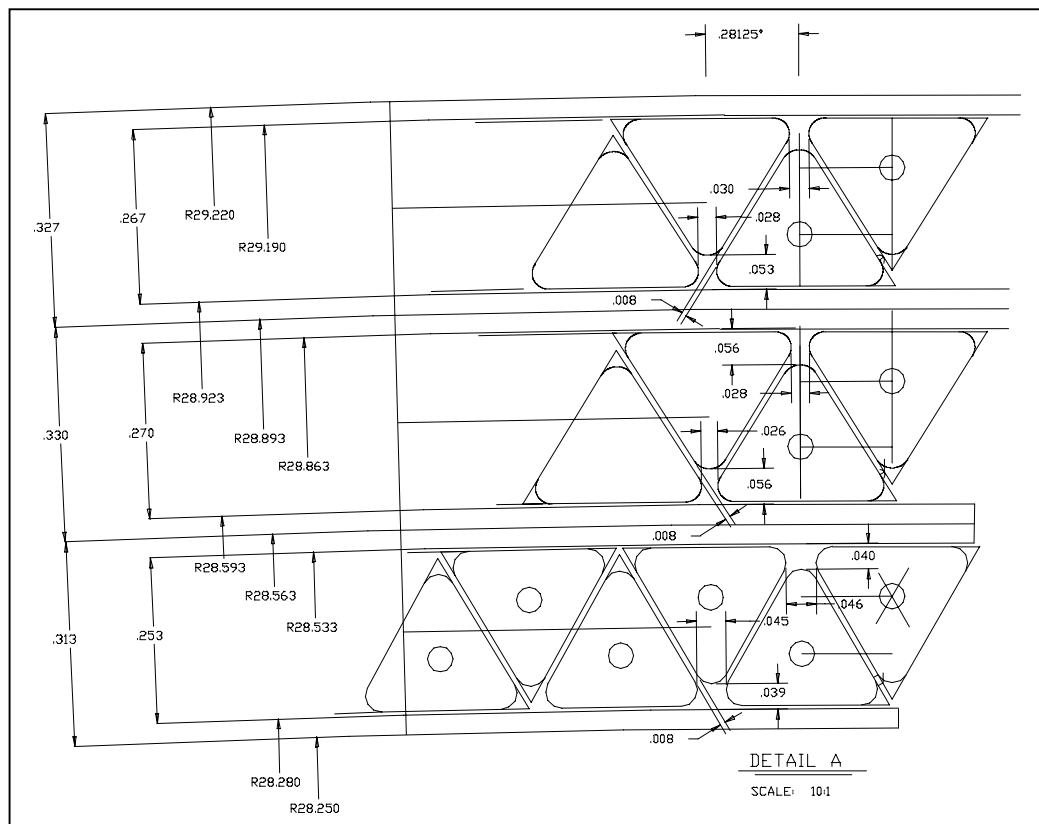


Figure 3. End view of the three CPS layers. Layers are axial, u, and v stereo in increasing radius. Note the change in strip to strip spacing in the three layers to accommodate the similar channel count of each layer.

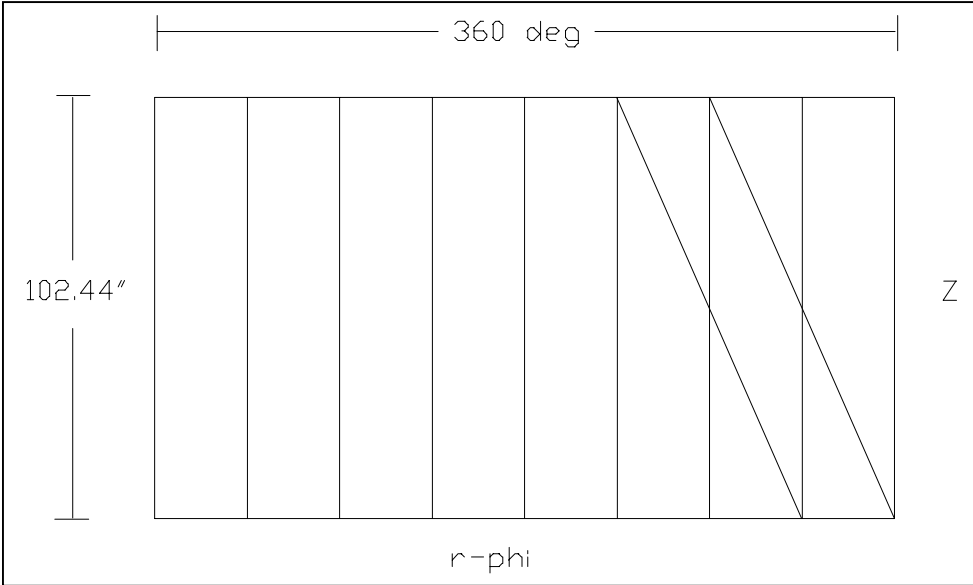


Figure 4. A “rolled out” depiction of the CPS axial layer and one inner stereo octant. This view is looking at the outer detector surface.

2. Detector Structure and Layout.

The CPS consists of three concentric cylindrical layers. In the following the layers are referred to as axial, inner stereo, and outer stereo. The axial layer is at the inner radius.

To facilitate detector construction, each CPS layer is formed from eight octant “modules”. The modules consist of two 1/32” stainless steel “skins”, with the triangular scintillator strips sandwiched between as seen in Fig. 3. The end region of two adjacent modules is shown in Fig. 5 .

The stereo modules are made such that their ends align to the ends of alternating axial modules. A “rolled out” depiction of the eight axial modules and one inner stereo module is shown in Fig. 4. The outer stereo modules rotate in the opposite direction as the inner stereo. The sign of the helicity of the inner stereo modules is such that when facing either readout end, the edge of the module rotates counter clockwise as Z increases.

The modules affix to the solenoid by bolts at each corner. Additionally eight 1/4” pins are placed on each end of the solenoid to provide registration. Stainless steel (ss) corner blocks are spot welded between the ss skins and have the holes for mounting and alignment made in.

On each module, one corner has a pin hole and the other corner on the same side has a pin slot. The side of the module with the alignment hole/slot is referred to as the “good” side. The opposite side is then naturally referred to as the bad side, and should register itself against the good side of the next module. Due to construction details the strip to strip spacing seen in Fig. 3 was smaller than the design value by ~ .0003, which leads to a ~.05” gap between modules. This is discussed further in section 6.

The ss connector blocks seen in Fig. 5 are also spot welded between the ss skins. This provides needed structural integrity in the end region of the modules. The connector blocks contain four holes, each tapped for 4-40, for mounting the WLS connector and a boot that covers the clear light guide connector.

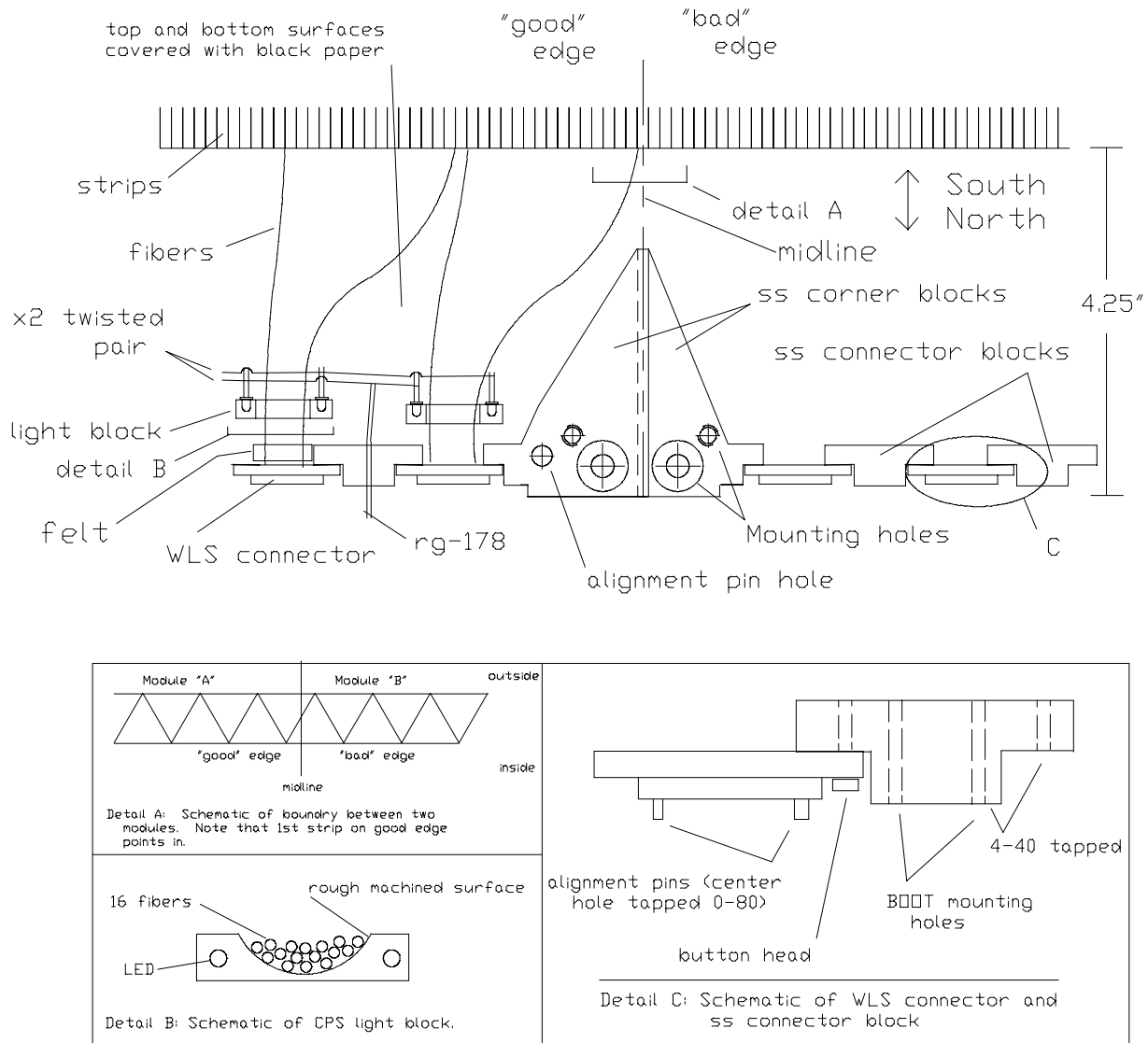


Figure 5. Schematic drawing of the components in the end region of two adjacent CPS modules.

Each bundle of WLS fibers runs over a light block as seen in Fig. 5. A cross sectional view is given in detail B. The light block is machined of lexan. Two blue LED's are mounted into either side, and are electrically isolated. Like side LED's from all 10 light blocks are chained in series.

Two rg-178 cables are connected to either LED string, and extend through the ss connector blocks on either edge of the module. The light block is made with a rounded shape to increase light transmission into the central region, but does not uniformly couple light to all 16 fibers.

The region between the back of the connector blocks and the end of the scintillator is enclosed in black paper. The paper is glued to the bottom skin. The top piece of paper is placed over the end region after all parts are installed, and is secured by tape. A strip of black felt is also wrapped around the wls fibers immediately behind the WLS connector to aid in light tightening. A small bead of epoxy was placed on the surface

of the ss blocks prior to gluing the top skin on. The bead was placed at the rear edge (closest to the scintillator) of all blocks and was to provide additional light tightening as the spot welding of the skin to the ss blocks did not insure a light tight seal.

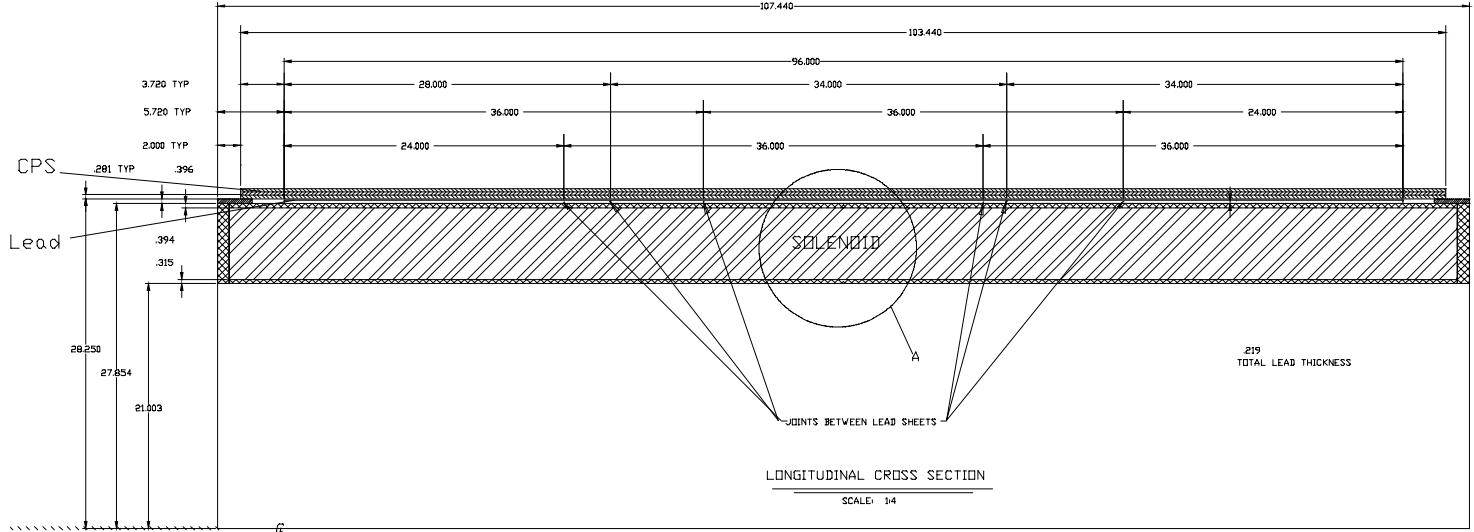


Figure 6. Cross sectional view of the solenoid, lead, and CPS with relevant dimensions.

The Pb pre-radiator is situated between the CPS and Solenoid. The pre-radiator is formed from long Pb sheets of thickness 1/32" and width 24" or 36". The final thickness of 7/32" was formed by gluing 7 layers of Pb to the solenoid with the joints as indicated in Fig. 6. The joints between layers were staggered. There was typically a space of 0 to 1/32" in any joint. In order to secure the Pb against any possible failure of the glue, a .02" thick ss sheet was tightly wrapped around the completed assembly and tack welded to itself.

Table 1 summarizes various quantities of interest for the CPS.

	axial scintillator	inner stereo scintillator	outer stereo scintillator	pb	stainless steel skins	alignment pin holes
ΔZ	94.94"	94.94"	94.94"	96"	103.44"	102.44"
Radial thickness	.253"	.27"	.267	7/32"	1/32" each	
average radius	28.407"	28.728"	29.057"			
stereo angle ¹		23.774 deg.	24.016 deg.			

¹ The stereo angle of each layer is given for the average radius. Note that the stereo angle within a each layer varies depending on radius and is given by the formula $\theta = \arctan ((\text{radius} * \pi / 2) / 102.44)$.

Table 1. Various dimensions of interest for the CPS and Pb pre-radiator.

3. Connector Channel Ordering

The strip to WLS connector hole mapping is shown in Fig. 6. The WLS connector connects to the clear fiber connector by two pins of dissimilar diameter. The pins provide for precision alignment of the connectors, and allow the connection to be made in only one way.

Two “rules” were used during WLS fiber bundle production.

1. When viewing either end of a module, and the module is concave down, the big pin is on the right.
2. When mapping the fibers between the strips and WLS connector holes, the strip closest to the good edge goes in the hole closest to the good edge.

This necessitates that the North and South clear light guides are not interchangeable. On the North end of a CPS module, strip #1 is in the WLS connector hole closest to the big pin, and on the South, strip #1 is in the hole closest to the small pin.

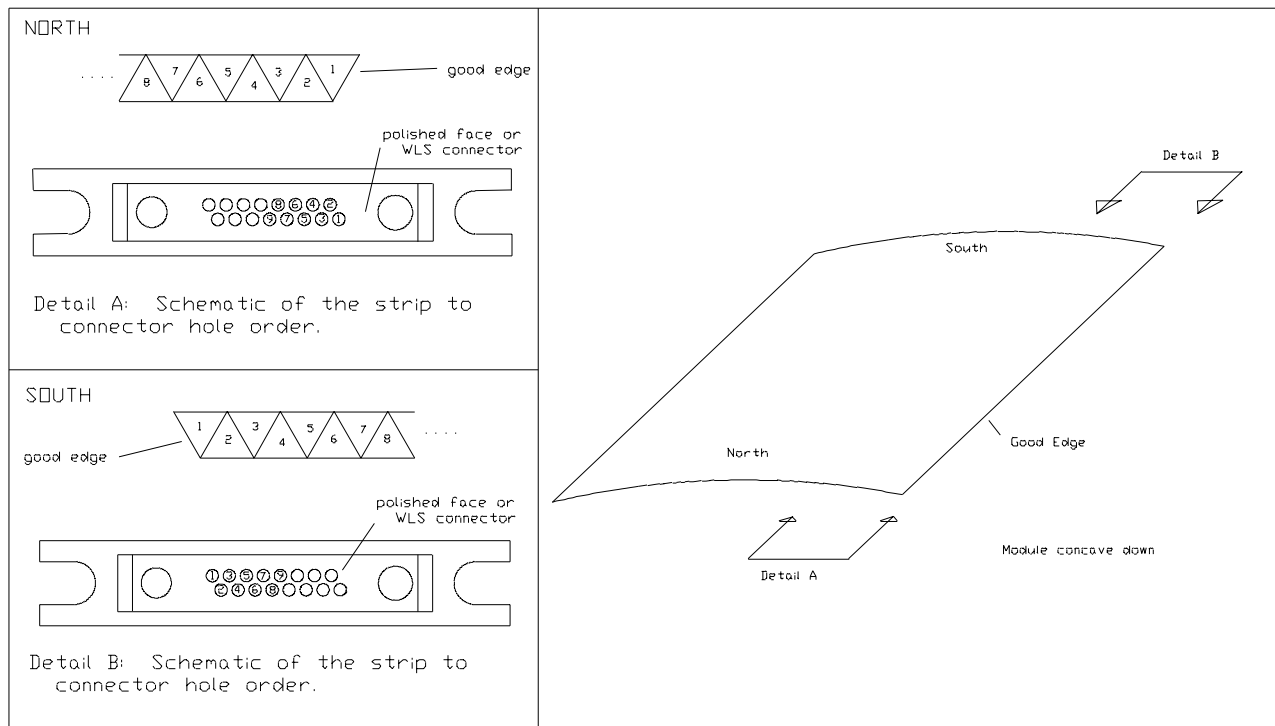


Figure 6. Schematic diagram showing the strip to WLS connector hole mapping on the North and South ends of the CPS.

4. Installation and final alignment of detector modules

The CPS was installed on the solenoid in April 98 prior to installing the solenoid in the Central Calorimeter. Eight ss pads were positioned on each end of the solenoid. The pads contained a hole for an alignment pin and also a $\frac{1}{4}$ -20 tapped mounting hole. The pads were roughed into position and secured with a ss strap running the full circumference of the solenoid. The ss strap was secured to the solenoid by pins to insure it would not rotate. A survey was then made of the alignment pin holes by the FNAL survey group, and the position of the pads was adjusted (typically with a rubber hammer) to the design positions. The RMS error in r-phi (from nominal) of the pin holes was $\sim .01''$. Following this procedure the pads were welded to the ss strap, and the position of the pin holes re-measured. The data from the final survey is summarized in table 2. Small deviations of the position of the pin holes were noted before and after welding. The typical accuracy of the survey equipment was $<.001''$.

Fig. 7 is a diagram of the 8 CPS sectors, viewed from the NORTH end of the solenoid. The angle theta is defined as increasing clockwise starting from the negative x axis. The alignment pins are placed such that the midlines between adjacent modules (see fig. 5) lie at the $0, 45, 90, \dots$ degree boundaries. The modules are built with the alignment hole placed 2.5 degrees from the midline. The nominal angles for the pins is thus $42.5, 87.5, 132.5, \dots$

The ΔZ between the north and south pins is nominally $102.44''$. By use of a hole/slot in the north/south corners (good side) of the modules, small deviations in ΔZ of the pins are tolerable. After the pins were installed, it was found that their ΔZ separation was short by $\sim 1/16''$, but this was within the tolerance afforded by the slot. However for purposes of stereo angle calculation, the value of $102.44''$ should still be used as the stereo modules were assembled based on this value and the systematic change on ΔZ of the pins does not change the angle of the modules wrt. the solenoid axis.

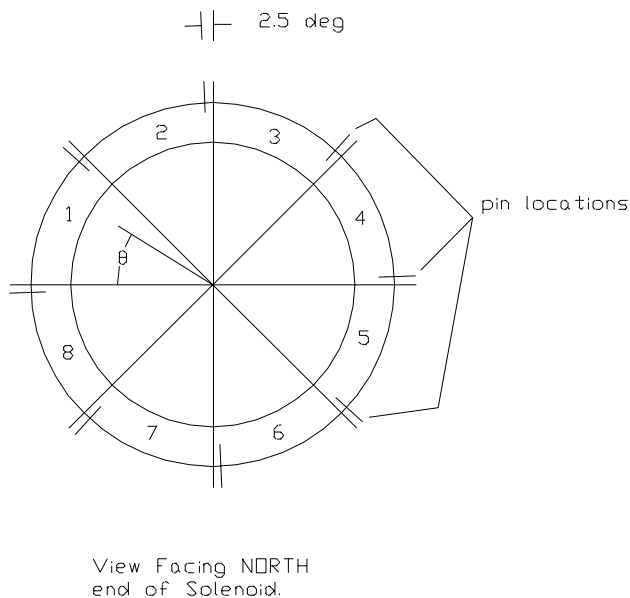


Figure 7. Diagram of 8 CPS sectors and coordinate system used for final survey. Theta is defined as increasing clockwise from the negative x axis. Nominal alignment pin location is -2.5 degrees from $0, 45, 90, \dots$

pin #	nominal θ (degrees)	actual θ (degrees)	delta θ (degrees)	delta r-phi ^T (inches) (@r=28.5")
NORTH				
1	42.5	42.538	.038	.019
2	87.5	87.502	.002	.001
3	132.5	132.481	-.019	-.009
4	177.5	177.494	-.006	-.003
5	- 137.5	-137.513	-.013	-.006
6	- 92.5	-92.496	.004	.002
7	- 47.5	-47.493	.007	.003
8	- 2.5	-2.465	.035	.018
SOUTH				
1	42.5	42.533	.033	.016
2	87.5	87.492	-.008	-.004
3	132.5	132.481	-.019	-.009
4	177.5	177.516	.016	.008
5	- 137.5	-137.476	.024	.012
6	- 92.5	-92.499	.001	.001
7	- 47.5	-47.487	.013	.007
8	- 2.5	-2.497	.003	.002

1. r-phi value correct to the nearest .001"

Table 2. The final survey positions of the CPS alignment pins, PRIOR to CPS module installation on solenoid.

5. Pre-installation Source Testing.

Prior to installation of the CPS onto the Solenoid, all 27 modules (9 of each type) were tested in a test stand in order to check for irregularities, dead channels, shipping damage, etc. The results of the test are summarized here for posterity. The testing was preformed in Jan-Feb of 1998. In general, the results were nominal for the entire system, with no major problems found.

The CPS was designed to be read out with high QE (70-80%) VLPCs. Typical response to a MIP is 20 VLPC pe's. Since commissioning and running of a VLPC cryostat would have been cost prohibitive, a system was devised to test the CPS modules using a strong Sr90 source and phototubes. A source must be used instead of cosmic rays as the typical MIP response for a phototube is only 2-3 pe's. By using a strong source, the light from a single channel can be routed to a PM tube, and the current drawn by the tube can be read out by a typical voltmeter.

Figure 8 shows a schematic of the test stand. A special fiber bundle is used to multiplex the 160 channels at one end of a module into 8 pm tubes. Each tube samples every 8th strip, 20 strips total. The current drawn by each tube is continuously (2 hz) read out into a pc through a GPIB bus. A rotating arm is used to slowly sweep the Sr90 source across the inside surface of a module. The arm would be positioned to the left of the bad edge of a module, the GPIB readout started, then the sweep was started. Sweep time was ~10 min. Two sets of 8 pm tubes and multiplexer fiber bundles were used at the north and south ends of a module, however, only one end was read out at a time. The source was swept near the ends of the fibers, approximately 2 inches from the nominal z=0 position (on either side).

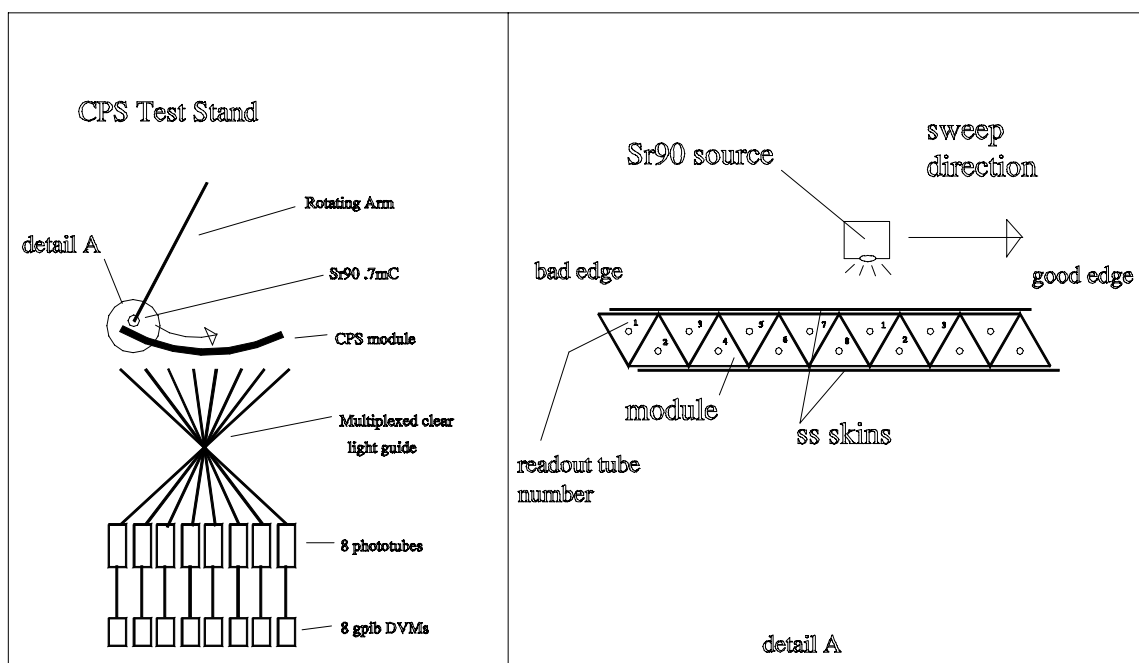


Figure 8. CPS test stand using a .7 mCurie Sr90 source. CPS readout is via a fiber bundle which multiplexes the 160 channels to 8 pm tubes.

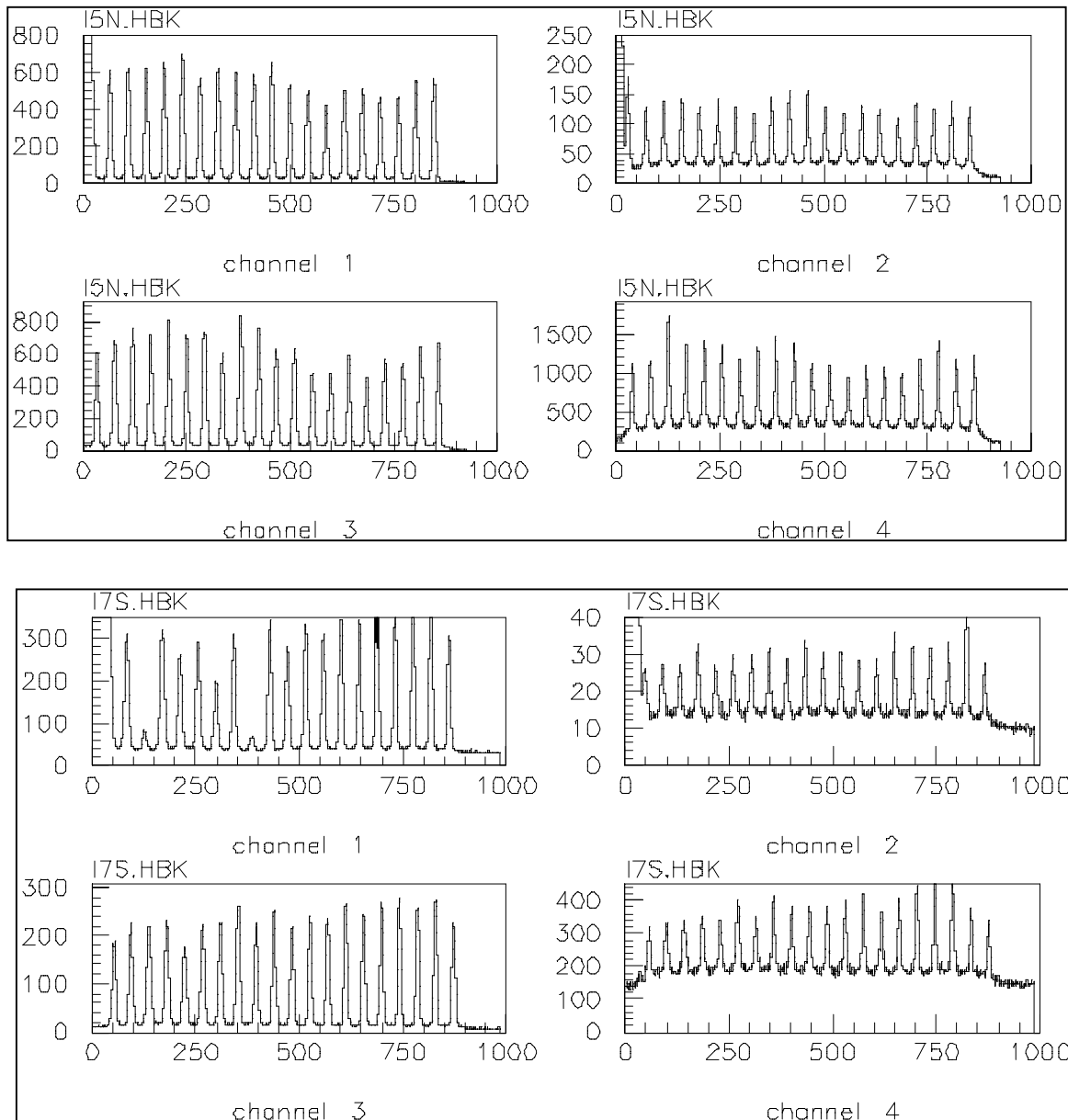


Figure 9. Raw data output of the tubes 1-4 for the north (top) and south (bottom) readout arrays. Plots on left are for top layer of strips and have better S/N ratio at peak than bottom layer of strips (plots on right).

Figure 9 shows typical raw output from the north and south pm tube arrays. Each plot corresponds to one pm tube. The y axis is relative and corresponds to the current draw of the tube, the x axis is the reading number, which corresponds to time. The twenty individual peaks are formed when the source is closest to each of the twenty strips read out by that tube. Edge effects can be seen in the first peak in channels (pm tubes) 1 and 2. These arise from the fact that the ss skin does not uniformly cover the scintillator strip as can be seen in Fig. 8.

The peak to valley ratio is seen to be better for the plots on the left had side in Fig. 9. The left hand plots read out the top layer of strips (see Fig. 8, detail A), and the right hand plots correspond to the bottom layer.

The dead channels seen in the plot I7S, channel 1, are from damaged fibers in the multiplexed fiber bundle, and are seen for all modules tested.

Since the source arm started its sweep at the bad edge of a module, peak 1 in channel 1 corresponds to CPS module channel 160 (channel number 1 is first strip on good edge), peak 1 in channel 2 corresponds to CPS module channel 159, etc..

The CPS strip to WLS fiber connector hole mapping can be checked with this data. Any mis-mapping would be of concern, particularly in the axial layer at the L1 trigger level. (The axial mapping was checked before the final skin was glued on, with one mis-mapped pair of fibers found for all 9 modules.) For a given sweep, and set of readouts for all 8 tubes, the location of the peaks were found, and plotted as a function of real channel number (as discussed above). A typical plot is shown in figure 10. Two mis-mapped WLS fibers would appear as a discontinuity in the line of points. Two such plots were made for each module (north and south end) and visually inspected for any mis-maps, with none found for all 27 modules.

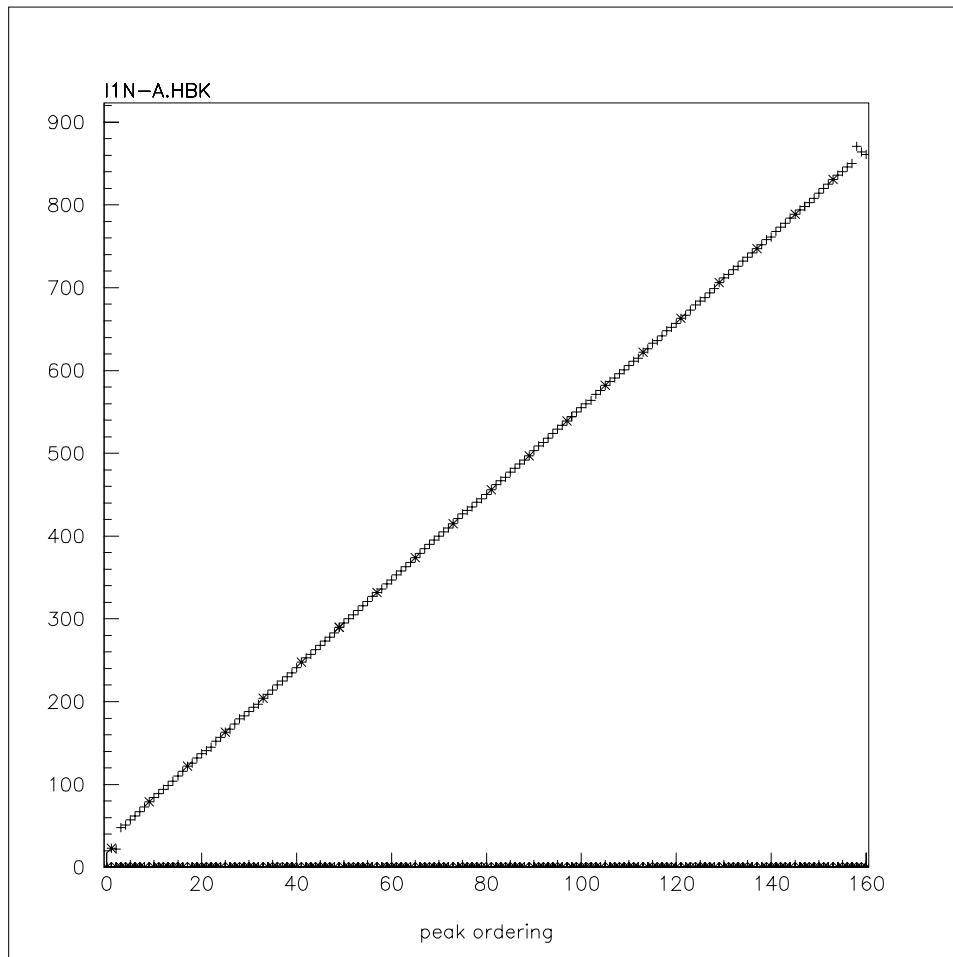


figure 10 Typical plot used to check the strip to WLS fiber connector hole mapping. The x axis is the channel number, and the y axis is the readout cycle number for the peak current draw for that channel. Irregularities on either end are from edge affects discussed in text. Mis-mapped strips would appear as a pair of points that did not lie on line.

In Figure 9, for any given channel, there is also a seemingly large rms variation between peak heights across the 20 peaks. This pattern is seen to repeat as different modules are cycled through the test stand. The large variation is assumed to be due to different couplings of the 20 clear light guide fibers to the pm tube. This can be seen in Fig. 11. This plot shows the peak heights of two readout tubes for the nine modules of a given type (in this case INNER STEREO), with each module represented as a different symbol.

A clear systematic can be seen. The error on any given data point is <1%. For tube 5, the spread of values (in a given cps channel) is characteristic of the expected strip to strip RMS variation (see ref 4 in (3)). In this plot, the 20 peak heights for each module are background subtracted, normalized such that their average is 1, and then data from all nine inner stereo modules are overplotted. In this data, tubes 5,6 read out a top,bottom layer of strips (see fig 9). The rms in a given channel is clearly larger for the tube 6 data. This is thought to arise from differences in the thickness of epoxy that the beta's must penetrate to reach the bottom strips. Epoxy tended to settle (non-uniformly) in the small space at the top of the bottom layer of strips (see fig. 3) during construction.

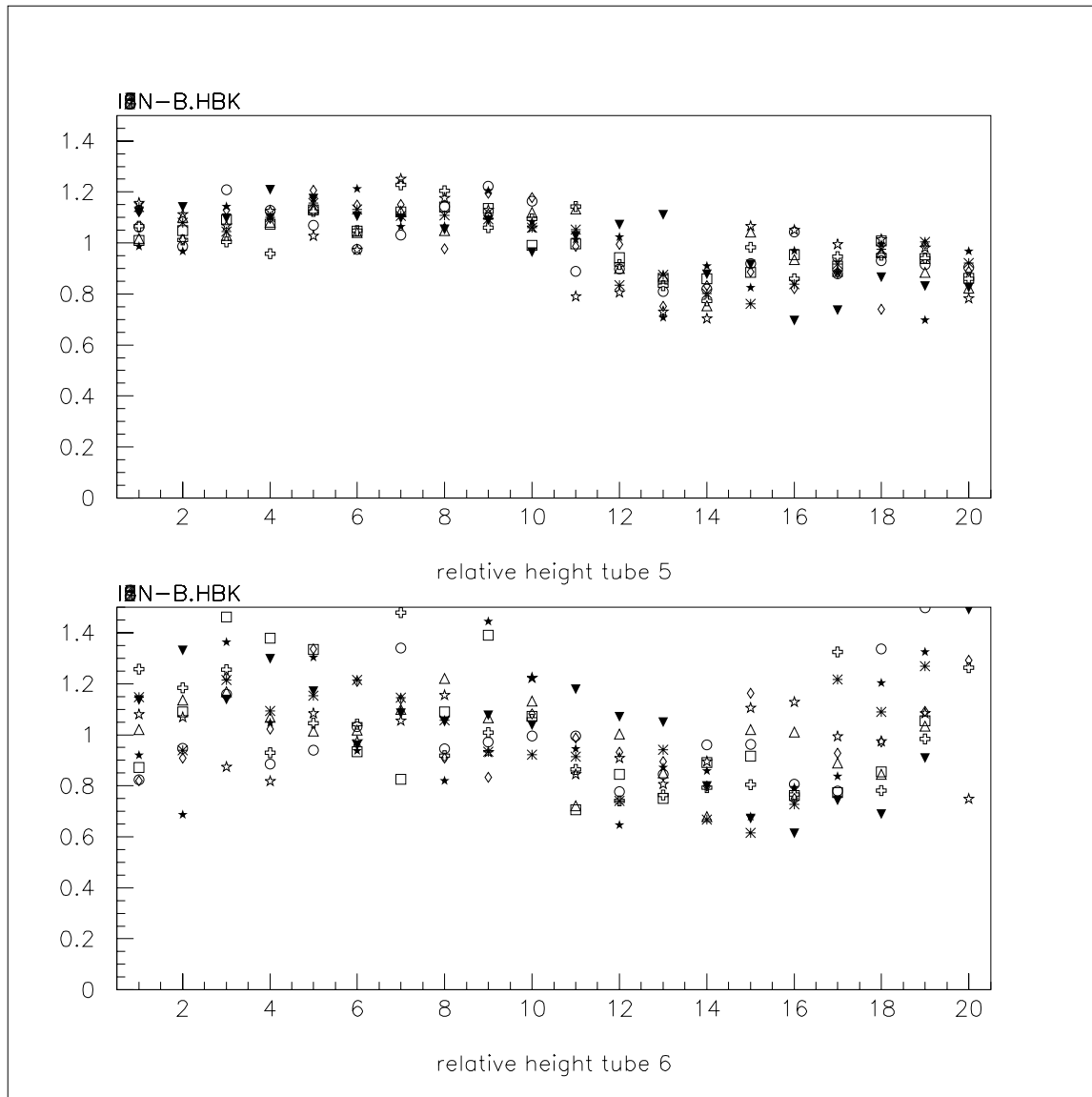


Figure 11. The relative peak heights in tubes 5 and 6 for all nine Inner Stereo (north end) modules tested. Data from the nine modules are overplotted as different symbols. The peak heights in a given tube, for each module, are normalized such that their average is 1.

An initial strip to strip calibration can be performed with this data. This will necessarily be a rough estimate of the strip to strip variations, but may be useful for a starting point for a run time calibration. Also, the bottom layer of strips will have larger errors (~ factor 2) based on their larger rms seen in Fig. 11. It is assumed that the rms seen for the top layer of strips will be typical for mips and showers.

Given the systematic trend of the average values in each of the 20 channels seen in Fig. 11, an additional calibration is loosely justified, namely to normalize the 9 data points in each channel such that their average is one. Typical distributions for top and bottom layers are given in Fig. 12.

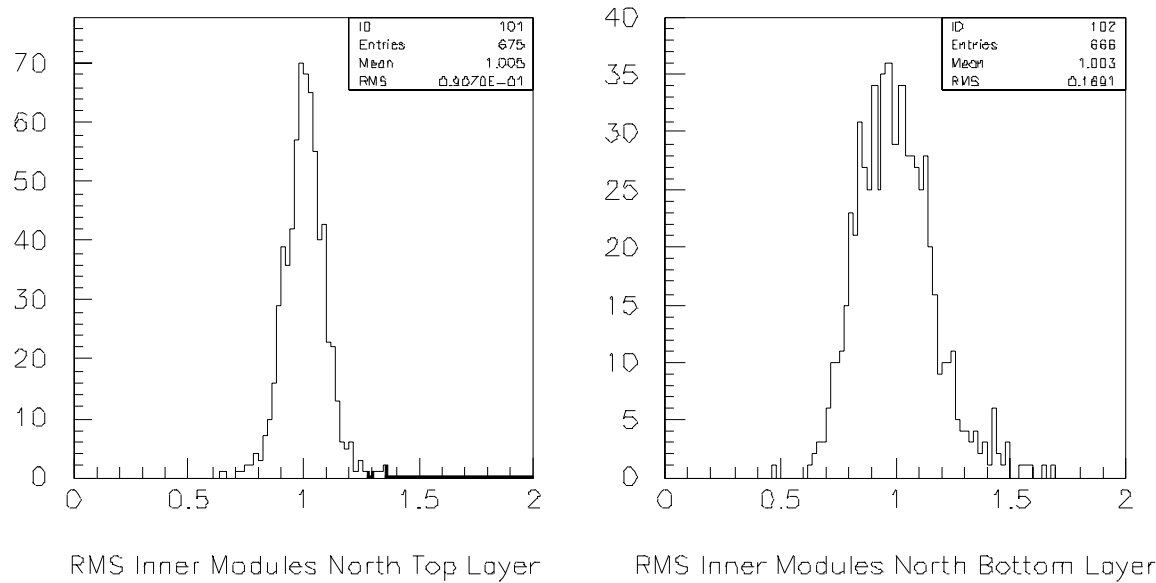


Figure 12. RMS deviation of the peak height for all CPS strips in the nine Inner Stereo modules, North end. Channels near module edges (2 or 3 channels on both sides) are not used due to edge effects. Peak heights are first background subtracted, then the 20 peak heights from a tube are normalized such that their average is 1 (to account for pm tube gain variations throughout test period), and finally the peak heights seen for the same channel in all nine modules are normalized such that their average is 1 (to account for systematics in the coupling of each channel to the pm tube).

With each CPS channel calibrated as above, a table of calibration constants for each strip can be made. The numbering of the modules, in the table below, corresponds to their production number. The mapping of modules onto the solenoid is given in the following tables. In the following tables, channel number 1 corresponds for the first strip on the good edge of a module. Note that the odd numbered channels correspond to the bottom layer of strips (see Fig. 8), and have a larger spread of values. In the following, readout channels that were unusable, either due to edge effects or broken clear light guide fibers, are represented as a -1. The Axial modules were all tested with the original pmt/multiplexer fiber bundle system and have similar dead channels. The south stereo

6. Minutia

This section contains still more scattered facts taken from the CPS construction logbook and other places that should be of interest when doing future CPS analysis.

Table 3 lists the mapping of the CPS module production number to the solenoid sector number (given in figure 7). After the source testing, broken fibers in modules axial-1 and outer-3 were identified and these modules were not installed.

sector (see fig. 8)	axial (production module #)	inner stereo	outer stereo
1	7	3	6
2	5	1 or 2	4
3	8	6	5
4	-	5	2
5	-	9	1
6	4	8	8
7	-	4	9
8	6	7	7

As mentioned in section 2, the module arclength was approximately 50 mills shorter than the design arclength. This was due to a systematic in the machining of the polystyrene jigs which where used to position the bottom layer of strips. At the time of manufacture, the time delay required to remake the jigs was schedule prohibitive, and the jigs were used as is. At the time of detector installation, typical gaps between the axial modules were $\sim .04''$, measured at either end. Note that the modules will sag up to $\sim .03''$ at their centers. This displacement is typically in the radial direction and depends on the module orientation.

This thickness of the scintillator portion of the module cross section came out $\sim .020''$ smaller than the design dimension. (see Fig. 3.). In the axial, the design thickness was $.253''$, and in production came out to be $\sim .235''$. This helps offset the arclength problem discussed above for the outer 2 layers.

References:

1. The D0 Upgrade, FERMILAB-Pub 96/357-E.
2. Design Report of the Central Preshower Detector for the D0 Upgrade, D0-Note 3014.
3. Forward and Central Preshower Detectors for the D0 Upgrade, Proceedings of the SCIFI 97, Conference on Scintillating Fiber Detectors, 1997, and references therein.

Appendix A:

The following postscript files contain the raw data from the CPS source test. To view the data double click on the icon from within MS word/



Ax.ps



In.ps



Out.ps

